AWARD NUMBER:

W81XWH-15-1-0073

TITLE:
Development of Tethered Hsp90 Inhibitors Carrying Radioiodinated Probes To Specifically Discriminate and Kill Malignant Breast Tumor Cells

PRINCIPAL INVESTIGATOR: Michael R. Zalutsky, Ph.D.

CONTRACTING ORGANIZATION: Duke University
Duke, NC 27710

REPORT DATE: May 2017

TYPE OF REPORT: Annual

PREPARED FOR: U.S. Army Medical Research and Materiel Command
Fort Detrick, Maryland 21702-5012

REPORT DOCUMENTATION PAGE

Form Approved
OMB No. 0704-0188

1. REPORT DATE	2. REPORT TYPE	3. DATES COVERED
May 2017	Annual	1May2016 - 30Apr2017

4. TITLE AND SUBTITLE
Development of Tethered Hsp90 inhibitors carrying Radioiodinated probes to specifically discriminate and kill Malignant breast tumor cells.

5a. CONTRACT NUMBER

5b. GRANT NUMBER
W81XWH-15-1-0073

5c. PROGRAM ELEMENT NUMBER

6. AUTHOR(S)
Michael Zalutsky
Timothy Haystead

E-Mail:Michael.zalutsky@duke.edu

5d. PROJECT NUMBER

5e. TASK NUMBER

5f. WORK UNIT NUMBER

7. PERFORMING ORGANIZATION NAME(S) AND ADDRESS(ES)
Duke University,
Office of sponsored research, 2200 W. Main Street, Suite 710
Box 104010,
Durham NC 27710

8. PERFORMING ORGANIZATION REPORT NUMBER

9. SPONSORING / MONITORING AGENCY NAME(S) AND ADDRESS(ES)
U.S. Army Medical Research and Materiel Command
Fort Detrick, Maryland 21702-5012

10. SPONSOR/MONITOR'S ACRONYM(S)

11. SPONSOR/MONITOR'S REPORT NUMBER(S)

12. DISTRIBUTION / AVAILABILITY STATEMENT
Approved for Public Release; Distribution Unlimited

13. SUPPLEMENTARY NOTES

14. ABSTRACT
We have proposed to develop tethered Hsp90 inhibitor capable of carrying various radioactive iodine isotopes for early detection and ablation of metastatic breast cancers. These probes specifically target a surface form of heat shock protein 90 (eHsp90) that is expressed on malignant cells and internalized. In this report we describe our chemistry efforts to synthesize a non-radioactive tethered Hsp90 inhibitor and methods developed for stannylation of the molecule such that it can be effectively radioiodinated with either ^{131}I or ^{124}I. Two paths of synthesis were developed and optimized. A standard operating procedure was developed and then adapted and modified to provide workable protocols for radioiodination. An inactive control molecule was also developed, which can also be labeled with radioiodine to permit determination of specificity of radio-ligand localization. These molecules will be tested as imaging agents in mouse models of breast cancer.

15. SUBJECT TERMS
Radiodination, tethered Hsp90 inhibitor, malignant breast tumor, ectopic Hsp90

16. SECURITY CLASSIFICATION OF:			17. LIMITATION OF ABSTRACT	18. NUMBER OF PAGES	19a. NAME OF RESPONSIBLE PERSON
a. REPORT	b. ABSTRACT	c. THIS PAGE			USAMRMC
Unclassified	Unclassified	Unclassified	Unclassified	16	19b. TELEPHONE NUMBER *(include area code) 919 613 8606*

Table of Contents

Page

1. Introduction

In the US, routine breast cancer screening results in over 1.6 million biopsies annually leading to the diagnosis and surgical resection of breast cancer or breast carcinoma *in situ* in over 250,000 women respectively. Unfortunately, the sensitivity but low specificity of screening has led to concerns about over treatment of indolent disease, as evidenced by the increased incidence and treatment of early stage breast cancer without a concomitant decrease in the nearly 40,000 breast cancer deaths annually. Clinical data indicate a strong link between high expression/activation of Heat shock protein 90 (Hsp90) with poor prognosis in malignant breast cancer (Cheng et al., 2012; Pick et al., 2007). Specifically, immunohistochemical analysis of breast cancer cell lines and 655 primary breast cancers (including 331 ER+ and 324 ER- tumors) showed increased Hsp90 expression in all breast cancer cell lines, and in nearly 90% of primary breast cancers (Pick et al., 2007). A recent study at our institution evaluated Hsp90 gene expression from profiles of over 4,000 breast cancer patients from 23 publically available gene expression databases, which also reported overall survival data from over 1000 patients. This study confirmed up regulated Hsp90 was associated with poor overall survival in all breast cancer subtypes including estrogen (ER) negative, HER2 negative and triple negative breast cancers (Cheng et al., 2012). Our laboratories recently developed a series of optical and iodinated tethered Hsp90 inhibitors that have exquisite selectivity *in vivo* for metastatic breast tumors expressing ectopic (cell surface) Hsp90 (Jared J. Barrott, 2013). We also discovered that ectopically expressed Hsp90 is rapidly internalized and can carry these tethered inhibitors specifically into the breast cancer cells. This work in tandem with published clinical results suggests that selective targeting of Hsp90 up regulated in malignancy may present an opportunity to not only discriminate indolent tumors from metastatic disease, but also offer a molecularly targeted radiotherapy approach for body wide tumor ablation with low normal tissue toxicity. Herein, we propose to develop a series of tethered Hsp90 inhibitors capable of selectively delivering radioiodine (^{124}I and ^{131}I) or ^{211}At to malignant tumor cells. We envisage a process in which a patient, after standard of care breast exam, is first evaluated for malignancy vs. indolent disease by positron emission tomography (PET) imaging using ^{124}I-labeled tethered inhibitors. Then, in patients with malignancies detected in high contrast to normal tissues, targeted radiotherapy would be preformed at patient-optimized doses of inhibitor labeled with the β-emitter ^{131}I or the α-emitter ^{211}At. ***This is an attractive strategy for breast cancer*** *because the same molecules can be used to not only discriminate indolent disease from metastatic, but also enables selective tumor ablation on a personalized level, potentially mitigating life altering side effects commonly associated with current chemotherapeutics or radiation strategies.*

2. Keywords

Radioiodinated, Tethered Hsp90 inhibitor, malignant breast cancer, iododestannylation

3. Accomplishments.

Chemistry. In last year's report, we described the development of **HS-131,** a compound that offered the potential of dual modality imaging including elements for both fluorescent and PET detection. In this analogue, fluorescein was utilized as a fluorescent dye and was introduced using FITC. We developed methodology to prepare the compound with cold (non-radioactive) iodine and developed and compared the feasibility of several methods for introducing radioactive iodine into the compound template.

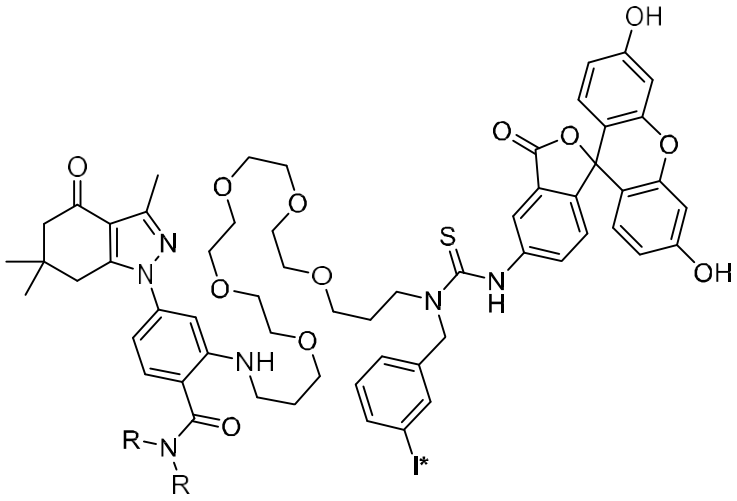

HS-131 R = H Target Fluorescent PET Agent
HS-212 R = CH_3 Inert control molecule

Because of some limitations related to the use of fluorescein, primarily related to background fluorescence in the same spectral region, we decided to evaluate the possibility of generating similar types of fluorescent compounds but that operated at longer wavelengths. We initially pursued the strategy of making iodinated analogs of some of our previously synthesized near IR probes that utilized cyanine dyes and emitted at 680 nm to 820 nm, depending on the individual dye structure. Detection of these dyes is much more sensitive and much less prone to interference. We have also generated a substantial body of data with these near IR probes, which will greatly facilitate the development of dual modality probes such as **HS-131**.

Initial approaches for introducing an aryl iodide template onto the **HS-131** template were unsuccessful. For example, Reductive amination, acylation and alkylation strategies all yielded multiple products in highly colored reaction mixtures. Finally, by repeatedly running a reductive alkylation reaction with sub-stoichiometric amounts of reducing agent followed by repeated chromatography, we could isolate about 11% of the desired product, at least by LC/MS.

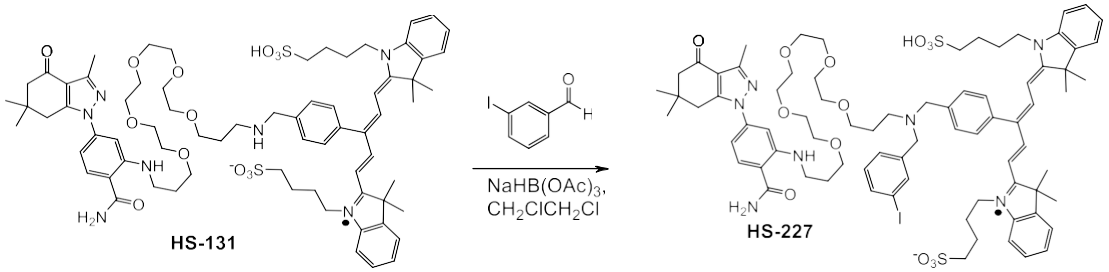

Unfortunately, numerous attempts to increase the yield or even reproduce the reaction were unsuccessful. However, with some of the product in hand that could

now be used as a standard, we returned to the alkylation reaction. By running the reaction in methanol, with solid sodium carbonate added as an insoluble base, the product was smoothly alkylated to give a product matching the product from reductive alkylation. After purification (59% isolated yield) away from some bis-alkylation, LC/MS and NMR confirmed the structure and the compound was registered as **HS-227**.

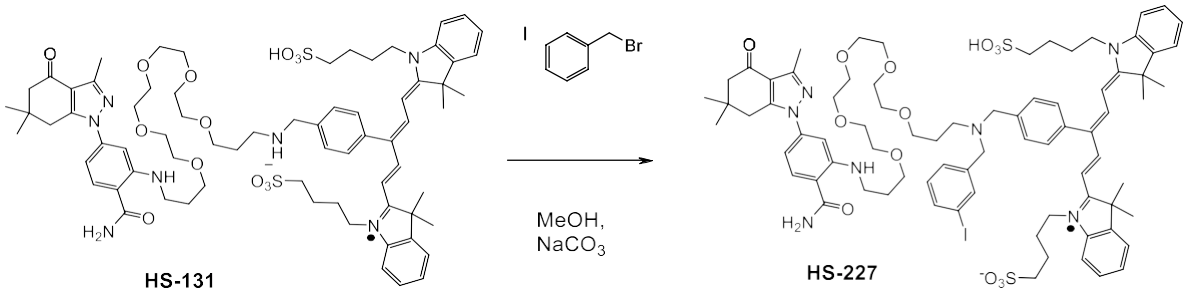

With useful quantities of **HS-227** now available, we were able to demonstrate its palladium mediated conversion to a trimethyltin analogue, the compound desired as a radiohalogenation precursor. We were then able to convert the compound back to the iodide. This conversion demonstrates the possibility of introducing other iodine isotopes into the molecule for PET imaging or perhaps even tumor ablation.

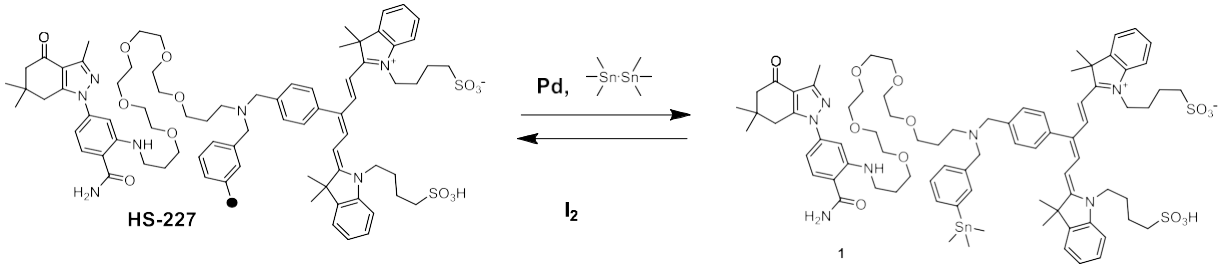

Using the identical alkylation methodological approach, we next made an iodo-analog of **HS-196** in good yield.

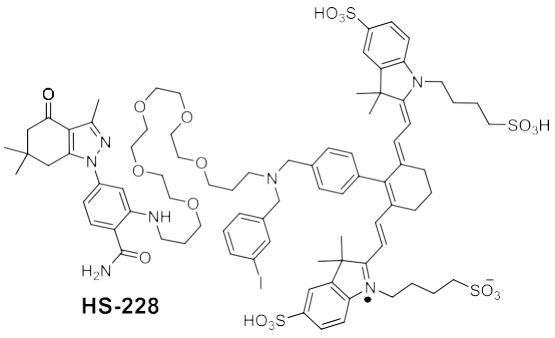

Although these results are encouraging, further work on optimizing the stannylation reaction is clearly needed. For example, a large quantity of proto-destanylation is seen in the reaction, which can be problematic. Moreover, the stannylation needs to be demonstrated on **HS-228**. Samples of **HS- 227** and **HS-228** were given to the Dr. Kim Lyerly's laboratory at Duke University Medical Center for imaging analysis evaluation experiments. Experimental details are provided the in the appendix.

Experimental Details

Unless otherwise stated, all reagents were obtained from commercial sources and used without further purification. Proton NMR spectra were obtained on Varian 400 and 500 MHz spectrometers. LC/MS were obtained on an Agilent ion-trap LC/MS system. High-resolution mass spectrometry results were obtained on an Agilent 6224 LCMS- TOF and are reported as an average of four runs. The syntheses of **HS-131** and compound **3** have been reported in the literature (Crowe et al., 2017). Dye **2** was obtained from Licor, Inc.

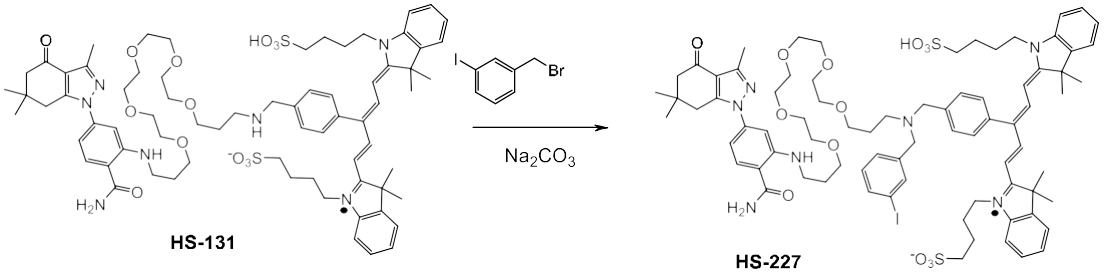

4-(2-((1E,3Z)-3-(4-(21-((2-carbamoyl-5-(3,6,6-trimethyl-4-oxo-4,5,6,7-tetrahydro-1H- indazol-1-yl)phenyl)amino)-2-(3-iodobenzyl)-6,9,12,15,18-pentaoxa-2-azahenicosyl)-phenyl)- 5-((E)-3,3-dimethyl-1-(4-sulfobutyl)indolin-2-ylidene)penta-1,3-dien-1-yl)-3,3-dimethyl-3H-indol-1-ium-1-yl)butane-1-sulfonate (HS-227). Compound **HS-131** (200 mg, 152 µmol), sodium carbonate (48 mg, 455 µmol) and 3-iodobenzyl bromide (59 mg, 197 µmol) were dissolved in methanol (8 mL) and stirred at RT for 20 h. The reaction mixture was then concentrated and chromatographed twice (150 g C-18, 0 to 100% MeOH with 0.2% formic acid) to give product **HS-227** (136 mg, 59%) as a blue solid. LC/MS shows a single peak with m/z = 767.8 $[M+2H]^{2+}$. ^{1}H-NMR (dmso-d_6) d 10.32 (br s, 1H), 8.47 (d, J = 14 Hz, 2H), 8.40 (br t, 1H), 8.03 (s, 1H), 7.93 (br s, 1H), 7.73-7.84 (m, 4H) 7.63 (d, J = 7 Hz, 2H), 7.35-7.43 (m, 6H), 7.26 (t, J = 7 Hz, 2H), 7.24 (d, J = 7 Hz, 2H), 6.76 (s, 1H), 6.67 (d, J = 7 Hz, 1H), 5.69 (d, J = 14 Hz, 2H), 4.46 (br m, 2H), 4.38 (br m, 2H), 3.82 (br m, 2H), 3.6-3.72 (m, 4H) 3.38-3.50 (m, 20H), 3.19 (m, 2H), 3.08 (m, 2H), 2.91 (s, 2H), 2.42 (m, 2H), 2.39 (s, 3H), 2.32 (s, 2H), 2.10 (m, 2H), 1.79 (m, 2H), 1.75 (s, 6H), 1.73 (s, 6H), 1.42-1.65 (br m, 8H), 1.00 (s, 6H).

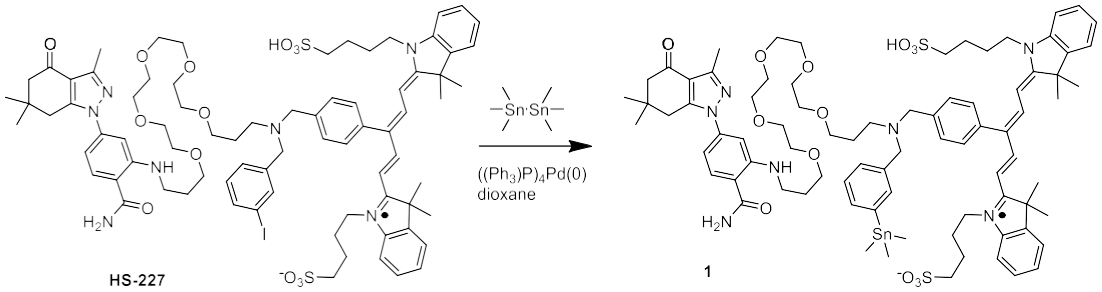

HS-227 (50 mg, 33 µmol), hexamethylditin (14 mg, 9 µL, 42 µmol) and tetrakis triphenylphosphine palladium(0) (1 mg 1 µmol) were slurried in dioxane (1 mL), purged with nitrogen for 30 m and heated to 100 ºC for an hour. The reaction was mixture was adsorbed onto silica gel and chromatographed (50 g C18, 0.2% formic acid to 100% MeOH) to give product **1** (13.9 mg, 27 %) as a blue solid. LC/MS gives a single peak with a little shoulder with m/z = 785.8 $[M+2H]^{2+}$ as part of a cluster typical of tin compounds. LC/MS was subsequently performed and unfortunately, showed significant decomposition, with the primary product being the hydride.

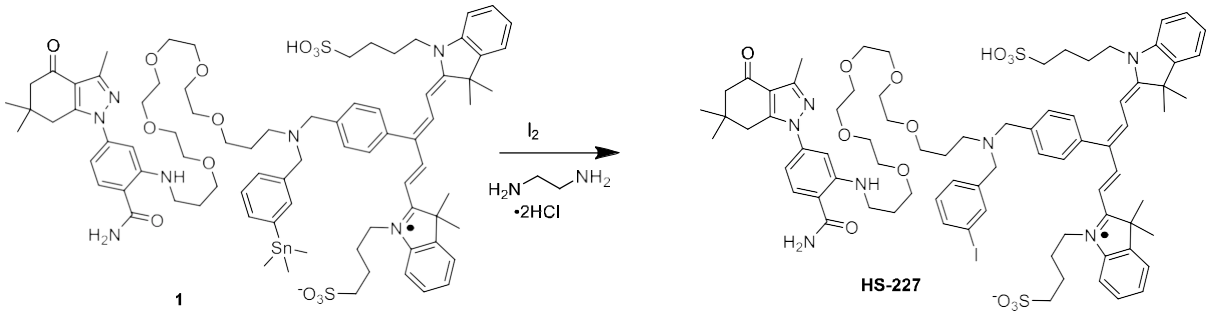

Protocol:

HS-227 and **1** were dissolved in methanol to make 1 mM solutions of both. A stock 100 mM solution of iodine in methanol was diluted 10-fold to give a 10 mM solution. A stock 1 M solution of ethylene diamine di hydrochloride in water was diluted 10-fold with methanol or water to give a 100 mM solutions. Six samples were prepared.

1. S1 50 µL of **HS-227** was diluted 10-fold with methanol. 500 µL total:
2. S2 50 µL of **1** was diluted 10-fold with methanol. 500 µL total.
3. S3 500 µL of **HS-131** 100 µM solution in methanol.
4. R1 50 µL of **1** was treated with 5 µL of 100 mM methanolic ethylenediamine dihydrochloride followed by 3 µL of 10 mM iodine solution. The solution was then diluted to 500 µL total.
5. R2 50 µL of **1** was treated with 5 µL of 100 mM aqueous ethylenediamine dihydrochloride followed by 3 µL of 10 mM iodine solution. The solution was then diluted to 500 µL tot.
6. R3 50 µL of **1** was treated with 5 µL of 100 mM aqueous ethylenediamine dihydrochloride followed by 3 µL of 10 mM iodine solution. This solution was left overnight and diluted to 500 µL the next day.

Samples S1, S2, S3, R1, R2, R3, were analyzed by HPLC (Zorbax Eclipse Plus C18 4.6 x 15 cm 5-micron. 30-minute linear gradient from 100% water with 0.2% formic acid to 100% methanol)

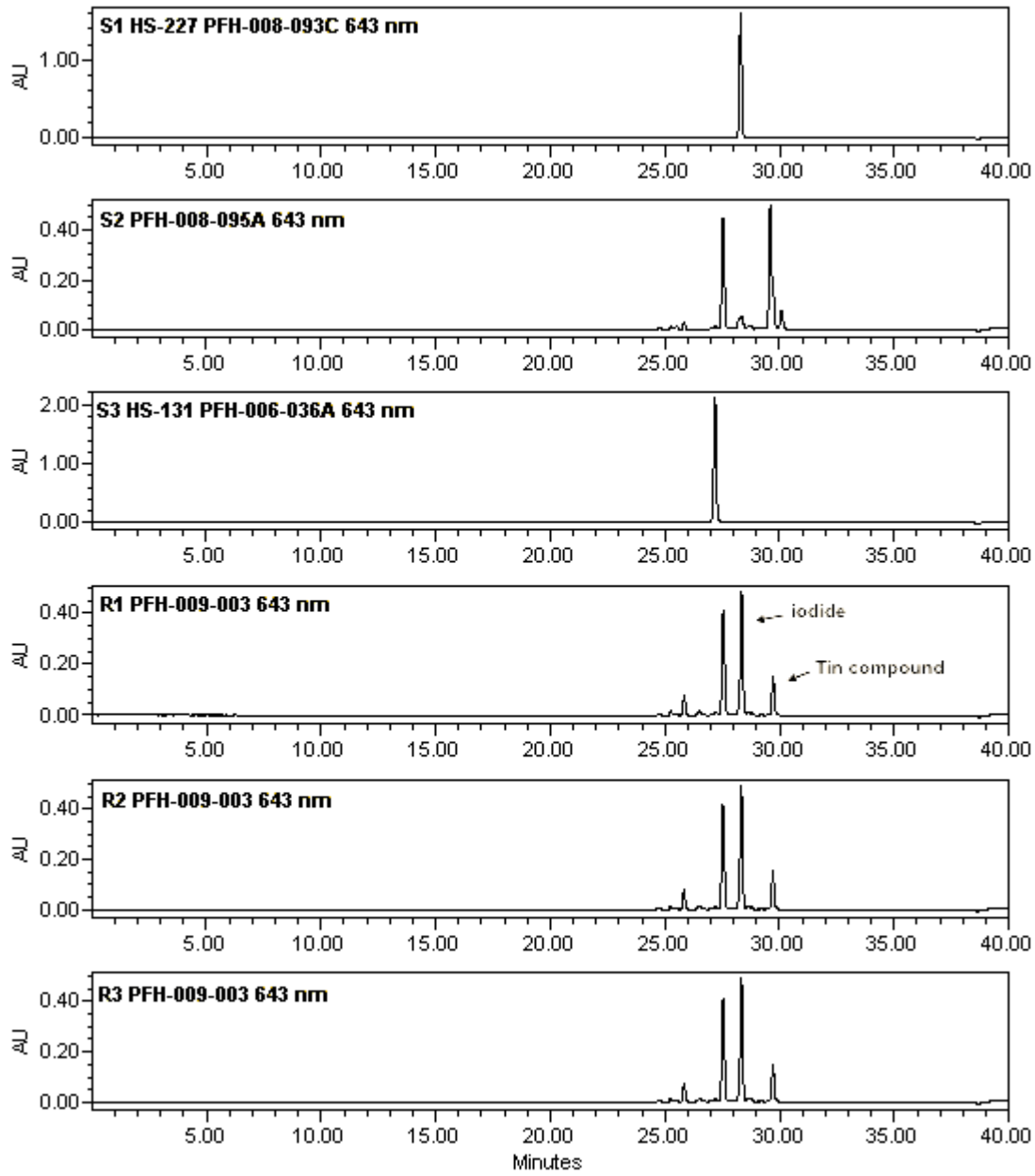

To show that the decomposition of **1** was not debenylation, **1** and **HS-131** were co-injected. Also, LC/MS showed no **HS-131.**

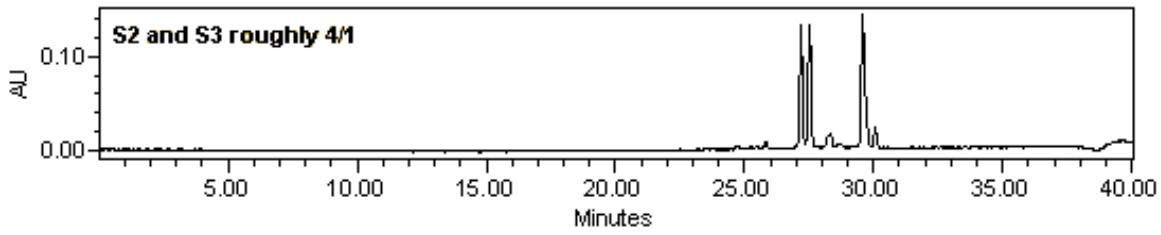

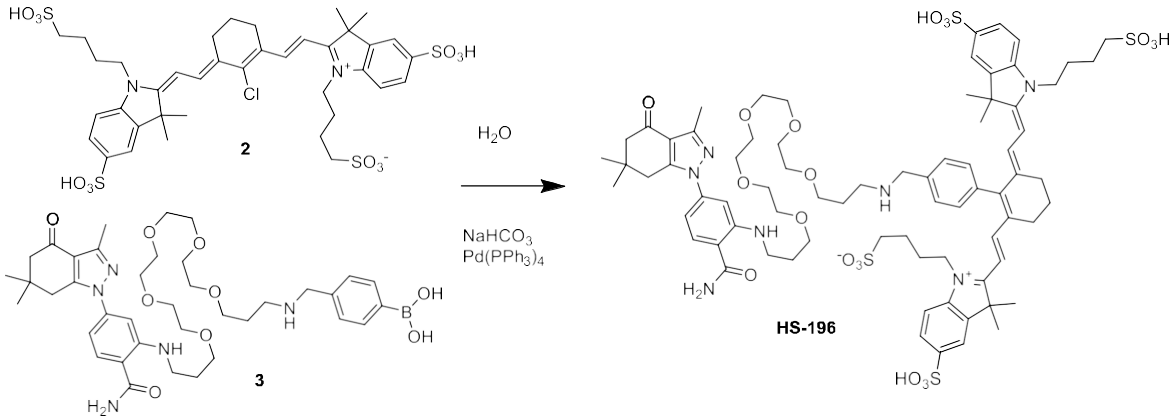

Phenylborate **3** (71 mg, 96 µmol), dye **2**, (85 mg, 95 µmol), tetrakis(triphenylphosphine) - palladium(0) (11 mg, 9.6 µmol) and sodium bicarbonate (46 mg, 431 µmol) were combined in water (2 mL), bubbled with N_2 for 30 min and heated to 100ºC for 1 h. The reaction mixture was dissolved in water and passed through Dowex-50 (2.75 g) onto an Isco 150 g C-18 column and chromatographed (0 to 100% MeOH in water) to give the product **108** (33.3 mg, 22%) as a dark green solid. LC/MS gave a single broad peak with m/z = 772.9 $[M+2]^{2+}$ and m/z = 771.0 $[M-2]^{2-}$. ^{1}H NMR NMR (DMSO-d_6) d 8.98 (br s, 2H), 7.74 (d, J = 8 Hz, 1H), 7.72 (d, J = 7 Hz, 2H), 756 (d, J = 7.0 Hz, 2H), 7.55 (s, 2H), 7.35 (d, J = 8 Hz, 2H), 7.28 (d, J = 8 Hz, 2H), 7.04 (d, J = 14 Hz, 2H), 6.77 (br s, 1H), 6.66 (d, J = 8 Hz, 1H), 6.23 (d, J = 14 Hz, 2H), 4.86 (v br, water), 4.38 (br t, J = 7.0 Hz, 4H), 4.05 (br m, 4H), 3.42-3.57 (m, 20H), 3.19 (t, J = 7.0 Hz, 2H), 3.07 (br m, 2H), 2.91 (s, 2H), 2.69 (br m, 4H), 2.51 (t, J = 7.0 Hz, 4H), 2.49 (DMSO), 2.38 (s, 3H), 2.32 (s, 2H), 2.01 (m, 2H), 1.94 (m, 2H), 1.79 (p, J = 7.0 Hz, 2H), 1.58-1.74 (br m, 8H), 1.12 (s, 12H), 1.00 (s,6H).

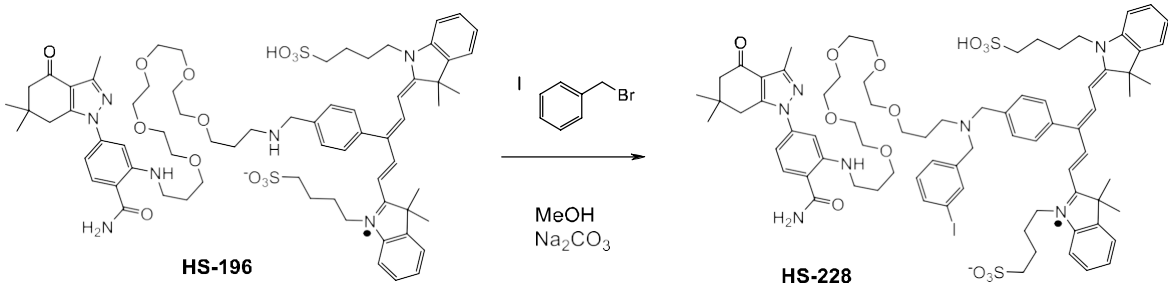

Compound **HS-196** (200 mg, 152 µmol), sodium carbonate (48 mg, 455 µmol) and 3-iodobenzyl bromide (59 mg, 197 µmol) were dissolved in methanol (8 mL) and stirred at RT for 20 h. The reaction mixture was then concentrated and chromatographed twice (150 g C-18, 0 to 100% MeOH with 0.2% formic acid) to give product **228** (136 mg, 59%) as a blue solid. LC/MS shows a single peak with m/z = 767.8 $[M+2H]^{2+}$. ^{1}H-NMR (dmso-d_6) d 10.32 (br s, 1H), 8.47 (d, J = 14 Hz, 2H), 8.40 (br t, 1H), 8.03 (s, 1H), 7.93 (br s, 1H), 7.73-7.84 (m, 4H) 7.63 (d, J = 7 Hz, 2H), 7.35-7.43 (m, 6H), 7.26 (t, J =

7 Hz, 2H), 7.24 (d, J = 7 Hz, 2H), 6.76 (s, 1H), 6.67 (d, J = 7 Hz, 1H), 5.69 (d, J = 14 Hz, 2H), 4.46 (br m, 2H), 4.38 (br m, 2H), 3.82 (br m, 2H), 3.6-3.72 (m, 4H) 3.38-3.50 (m, 20H), 3.19 (m, 2H), 3.08 (m, 2H), 2.91 (s, 2H), 2.42 (m, 2H), 2.39 (s, 3H), 2.32 (s, 2H), 2.10 (m, 2H), 1.79 (m, 2H), 1.75 (s, 6H), 1.73 (s, 6H), 1.42-1.65 (br m, 8H), 1.00 (s, 6H).

Imaging. Preliminary assessment of imaging properties if this novel potential tracer were assessed through a collaboration with University of North Carolina. These studies were performed at UNC under blanket imaging protocols in place at the Small Animal Imaging Core and with animals from the Mouse Phase 1 Unit, under their protocols. Methods for radiolabeling were transferred to UNC personnel and the imaging studies were performed with private funding.

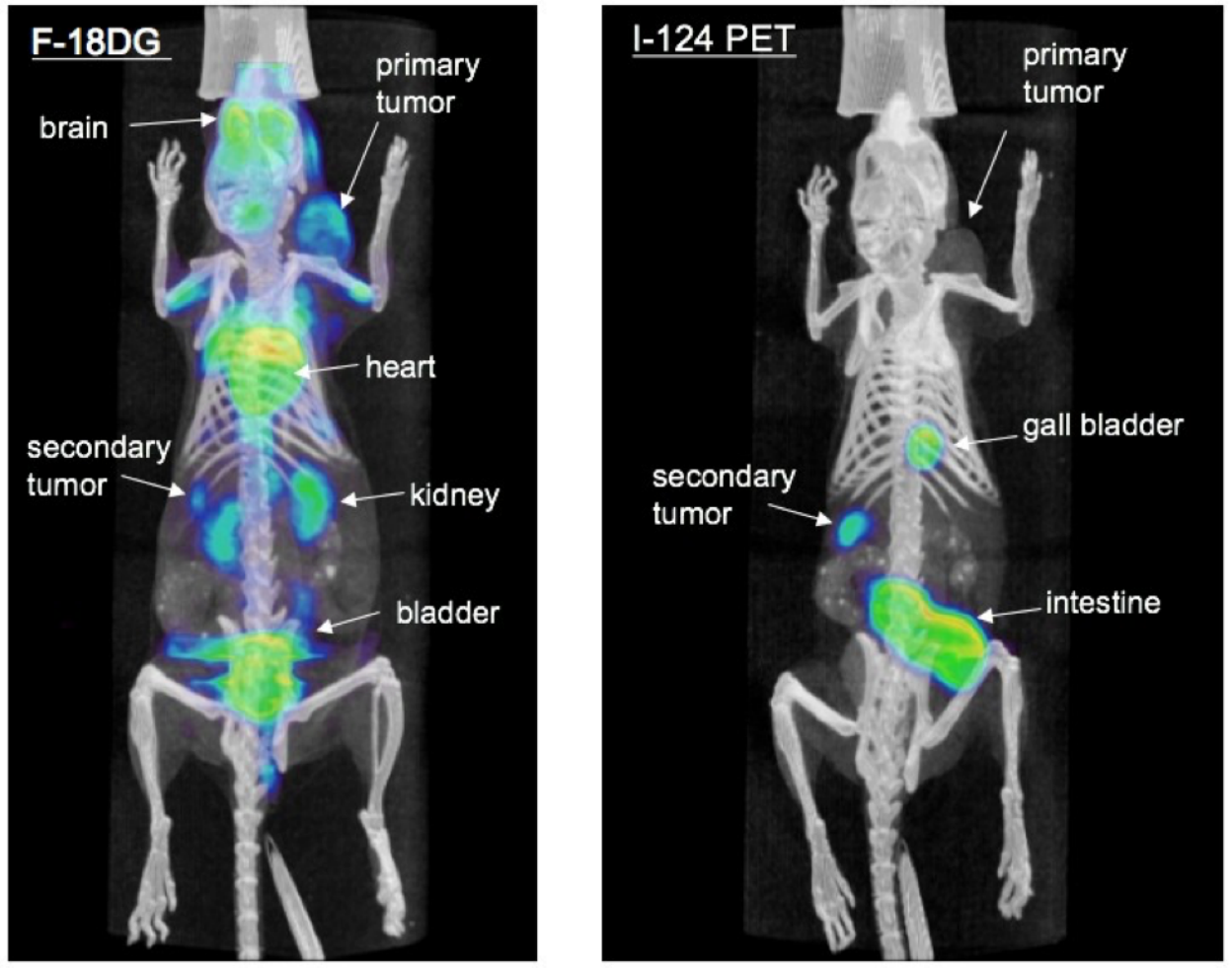

Figure 1. PET/CT comparison images of [^{18}F]FDG and ^{124}I-labeled HS-113, a tethered Hsp90 inhibitor. The MMTV-neu mouse first received [^{18}F]FDG via tail vein injection and images were obtained 60 min later. After 24 h, the same mouse received ^{124}I-labeled HS-113 via the same route and images were obtained after 60 min. In these images, the grey represents the CT image while the colored areas represent the distribution of the radiotracers.

For these studies, the MMTV-neu murine model of HE2-positve metastatic breast cancer was utilized. The sequence of events was: inject [^{18}F]fluorodeoxyglucose

([^{18}F]FDG; current gold standard for oncologic imaging by PET); wait 60 min and obtain microPET/CT images; wait 24 h and inject ^{124}I-labeled **HS113**; wait 60 min, image again. As shown in the left panel of Figure 1, [^{18}F]FDG was taken up by many normal tissues including the brain, eye, heart, lymph nodes kidney, liver and bladder. In addition, [^{18}F]FDG also was present in two tumors, both the large primary lesion located near the neck, and a smaller tumor located on the left flank and superimposed on the lowest rib. In contrast, ^{124}I-labeled **HS113** distribution at 60 min post injection was confined to the gall bladder, lower bowel and the smaller tumor located on/above/below the rib. It is interesting to note that the tumor appear larger on ^{124}I-labeled **HS113** imaging compared with [^{18}F]FDG in the same animal. We speculate that the lack of uptake of **HS113** in the primary tumor may reflect its necrotic state compared to the more actively growing secondary tumor. One of the most striking feature of **HS113** is its rapid clearance, nearly exclusively through the bile in comparison to all other fluorophore-tethered Hsp90 inhibitors that we have examined in tumor bearing animals. Without exception, elimination primarily occurs through the kidneys and urine. Whole body real time PET imaging over the first 30 min revealed the extent to which ^{124}I-labeled **HS113** is cleared by the hepatobiliary system. As shown in Figure 2, beginning at about 10 min after injection, the probe discriminates the outline of the liver and by 15-20 min, the architecture of the biliary ducts are revealed, until most the probe collects as an intense signal in the gall bladder. Finally, the radioactivity is delivered as a large bolus to the intestines.

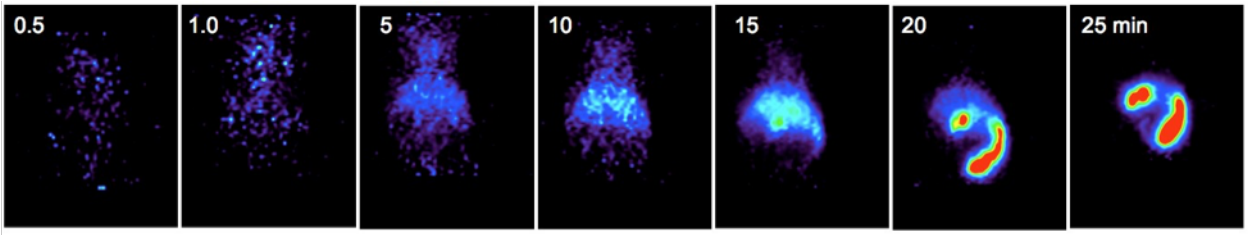

Figure 2. Images taken from dynamic imaging of ^{124}I-labeled HS-113 illustrating early phase pharmacokinetics after intravenous injection in a mouse.

4. Impact

Although there is clearly much work to be done to optimize this imaging strategy, the work accomplished during the past year is important because it demonstrates from a chemistry perspective that dual-purpose probes can be synthesized and labeled with ^{124}I. However, these imaging studies suggest that addition of the benzyl iodide alone dramatically alters the rate and route of probe clearance compared to prior fluorophore-tethered inhibitors. Two explanations may

explain this phenomenon, either the molecule is rapidly metabolized releasing the iodinated prosthetic or **HS-113** interacts in some manner with the hepatobiliary network via the benzyl iodide group.

5. Changes/Problems

With any chemistry program, one can anticipate encountering technical issues during the synthesis of a molecule. Major issues include poor yield, loss of solubility, unpredicted product formation, difficulties with selective iodination, stannylation, and/or radioiodination. Compounds that exhibit such behavior will not be pursued. One anticipated issue is the impact of the imaging moiety and its effect on cellular internalization of the probe where it can interact with normal tissue Hsp90 pools. Although we would still classify our tethered inhibitors as small molecules (average MW 800-1400 Da), they do fall outside of classically held rules of druggability such as Lipinski's rule of 5 (Lipinski, 2000). Indeed, generally our molecules are polar and have low cLogP values compared to PU-H71 and SNX5422, preventing them from freely diffusing into cells. In instances where the imaging moiety has a large impact on internalization, we will replace this with other fluorophore or iodine carrying functionalities. As discussed, we have observed that choice of these moieties dramatically effects the pharmacokinetic properties and clearance half time ($T_{1/2}$) of our tethered inhibitors from the tumor, and importantly, also the selectivity for Hsp90 binding. Generally, larger more polar moieties (e.g. fluorescein compared with NrIR versions slow the rate of elimination, whereas the addition of smaller molecules such as a benzyl group increases uptake. In many ways, defining which iodine or fluor carrying moiety is chosen will be an empirically driven process. We anticipate that our studies with cell lines will address such issues in advance of animal studies. However, we recognize that even the best performers in cell-based studies will behave unpredictably in animal. We believe on the imaging side there is sufficient diversity of commercially available fluorophors of varying structural diversity to enable us to define one or more tethered inhibitors that will meet our criteria. As discussed, an idealized tethered inhibitor will carry both radioiodine and a fluorophore, the latter enabling tumor cell selectivity within a biopsy to be determined by confocal microscopy. As indicated in this Progress Report, we have successfully synthesized at least one duel-imaging molecule, **HS113**, carrying fluorescein and iodine. In some respects, the fluorophores can be considered to be a surrogate for adding chemical bulk and diversity to our molecules for altering PK characteristics, with the added advantage of being

fluorescent.

We are somewhat limited in the diversity of the types of molecules that can carry iodine stably. Our current lead iodine carrying molecule is a benzylamine e.g. **HS-113**. The aryl-iodine in this molecule is predicted to be highly stable *in vivo* and unlikely to leach the incorporated iodine into the body where it could be taken up as free iodide in the thyroid and the stomach. Other obvious choices that carry iodine are not considered ideal, e.g. phenols and amino acids such as tyrosine (found in thyroxine) because of their propensity for undergoing deiodination because of the action of endogenous deiodinases. These are also less stable and likely to be metabolized in non-tumor tissues if not directly transported into the thyroid. However, if our benzylamide versions fail in animal studies because of rapid clearance from the circulation, phenols and amino acids such as tyrosine or phenylalanine offer alternate approaches. Another strategy for altering PK involves switching the ligand portion of the molecules to other Hsp90 inhibitors that may have higher affinity for Hsp90 or different PK properties than the HS-10 indoline scaffold e.g. Ganestespib and NVP-AUY922 (Eccles et al., 2008; Shimamura et al., 2012). If it becomes intractable to use iodine as a radio-label, we will explore the use of ^{18}F. This is the most commonly used radionuclide in clinical PET and has a much shorter half-life (100 min) compared with various radioisotopes of iodine which can range from a few days (^{124}I) to weeks (^{125}I). There are several strategies for incorporating ^{18}F, the most straightforward would be to use the methods of Vasdev (Rotstein et al., 2016), whereby iodine is directly activated for fluoride displacement. Another alternative would be to utilize one of several BODIPY dyes for imaging and use the methods of Li (Liu et al., 2014a) or Mazitschek (Hendricks et al., 2012) for ^{18}F displacement on the dye. A third approach would involve using an alternative labeling moiety based on a fluoride substitution or exchange on a boronate as reported recently by Perrin lab and coworkers (Liu et al., 2014b; Liu et al., 2014c).

6. Products

Several novel radio-iodinated tethered Hsp90 inhibitors have been developed that include iodine in their structure and have been successfully labeled with ^{124}I . Of these potential tracers, **HS113** currently shows the most promise in mouse models of human breast cancer as a novel PET imaging agent for noninvasive monitoring of HSp90 status in patients with this disease.

7. Participants & Other Collaborating Organizations……

Grants.gov ID Number	**W81XWH-15-1-0073**
Principal Investigator	**Timothy Haystead**
Performing Organization	**Duke University**
Contracting Organization	**Duke University**
Partner Budget Requested	**$549,500**
Direct Costs	**$350,000**
Indirect Costs	**$199,500**

8. Special Reporting Requirements

none

9. Appendices

none

References:

Cheng, Q., Chang, J.T., Geradts, J., Neckers, L.M., Haystead, T., Spector, N.L., and Lyerly, H.K. (2012). Amplification and high-level expression of heat shock protein 90 marks aggressive phenotypes of human epidermal growth factor receptor 2 negative breast cancer. Breast cancer research : BCR *14*, R62.

Crowe, L.B., Hughes, P.F., Alcorta, D.A., Osada, T., Smith, A.P., Totzke, J., Loiselle, D.R., Lutz, I.D., Gargesha, M., Roy, D.*, et al.* (2017). A Fluorescent Hsp90 Probe Demonstrates the Unique Association between Extracellular Hsp90 and Malignancy in Vivo. ACS Chem Biol *12*, 1047-1055.

Eccles, S.A., Massey, A., Raynaud, F.I., Sharp, S.Y., Box, G., Valenti, M., Patterson, L., de Haven Brandon, A., Gowan, S., Boxall, F.*, et al.* (2008). NVP-AUY922: a novel heat shock protein 90 inhibitor active against xenograft tumor growth, angiogenesis, and metastasis. Cancer research *68*, 2850-2860.

Hendricks, J.A., Keliher, E.J., Wan, D., Hilderbrand, S.A., Weissleder, R., and Mazitschek, R. (2012). Synthesis of [18F]BODIPY: bifunctional reporter for hybrid optical/positron emission tomography imaging. Angew Chem Int Ed Engl *51*, 4603-4606.

Jared J. Barrott, P.F.H., Takuya Osada, Xiao-Yi Yang, Zachary C. Hartman, David R. Loiselle, Neil L. Spector, Len Neckers, Narasimhan Rajaram, Fangyao Hu, Nimmi Ramanujam, Ganesan Vaidyanathan, Michael R. Zalutsky, H. Kim Lyerly, and Timothy A. Haystead (2013). Optical and Radioiodinated Tethered Hsp90 Inhibitors Reveal Selective Internalization of Ectopic Hsp90 in Malignant Breast Tumor Cells. Cell Chemistry and Biology *20*, 1-11.

Lipinski, C.A. (2000). Drug-like properties and the causes of poor solubility and poor permeability. Journal of pharmacological and toxicological methods *44*, 235-

249.

Liu, S., Li, D., Zhang, Z., Surya Prakash, G.K., Conti, P.S., and Li, Z. (2014a). Efficient synthesis of fluorescent-PET probes based on [(18)F]BODIPY dye. Chem Commun (Camb) *50*, 7371-7373.

Liu, Z.B., Pourghiasian, M., Radtke, M.A., Lau, J., Pan, J.H., Dias, G.M., Yapp, D., Lin, K.S., Benard, F., and Perrin, D.M. (2014b). An Organotrifluoroborate for Broadly Applicable One-Step F-18-Labeling. Angewandte Chemie-International Edition *53*, 11876-11880.

Liu, Z.B., Radtke, M.A., Wong, M.Q., Lin, K.S., Yapp, D.T., and Perrin, D.M. (2014c). Dual Mode Fluorescent F-18-PET Tracers: Efficient Modular Synthesis of Rhodamine- cRGD (2)- F-18 - Organotrifluoroborate, Rapid, and High Yielding One-Step F-18-Labeling at High Specific Activity, and Correlated in Vivo PET Imaging and ex Vivo Fluorescence. Bioconjugate Chemistry *25*, 1951-1962.

Pick, E., Kluger, Y., Giltnane, J.M., Moeder, C., Camp, R.L., Rimm, D.L., and Kluger, H.M. (2007). High HSP90 expression is associated with decreased survival in breast cancer. Cancer research *67*, 2932-2937.

Rotstein, B.H., Wang, L., Liu, R.Y., Patteson, J., Kwan, E.E., Vasdev, N., and Liang, S.H. (2016). Mechanistic Studies and Radiofluorination of Structurally Diverse Pharmaceuticals with Spirocyclic Iodonium(III) Ylides. Chem Sci *7*, 4407-4417.

Shimamura, T., Perera, S.A., Foley, K.P., Sang, J., Rodig, S.J., Inoue, T., Chen, L., Li, D., Carretero, J., Li, Y.C.*, et al.* (2012). Ganetespib (STA-9090), a nongeldanamycin HSP90 inhibitor, has potent antitumor activity in in vitro and in vivo models of non-small cell lung cancer. Clinical cancer research : an official journal of the American Association for Cancer Research *18*, 4973-4985.